THE JOURNAL OF BIOLOGICAL CHEMISTRY
Vol. 279, No. 50, Issue of December 12, pp. 50791–50802, 2003
Printed in U.S.A.
© 2003 by The American Society for Biochemistry and Molecular Biology, Inc.

CD38 Signaling in T Cells Is Initiated within a Subset of Membrane Rafts Containing Lck and the CD3-ζ Subunit of the T Cell Antigen Receptor*

Received for publication, July 23, 2003, and in revised form, September 22, 2003
Published, JBC Papers in Press, September 30, 2003, DOI 10.1074/jbc.M308034200

Pilar Muñoz‡§, María-del-Carmen Navarro‡¶, Esther J. Pavón‡‖, Javier Salmerón, Fabio Malavasi‡‡, Jaime Sancho‡, and Mercedes Zubiaur‡§§**

*From the ‡Instituto de Parasitología y Biomedicina, Consejo Superior de Investigaciones Científicas, 18001 Granada, the **Hospital Universitario San Cecilio, 18012 Granada, Spain, and the ‡‡Laboratory of Immunogenetics, University of Torino Medical School, 10126 Torino, Italy*

In this study we present data supporting that most CD38 is pre-assembled in a subset of Brij 98-resistant raft vesicles, which were stable at 37 °C, and have relatively high levels of Lck and the CD3-ζ subunit of T cell antigen receptor-CD3 complex in contrast with a Brij 98-soluble pool, where CD38 is associated with CD3-ζ, and Lck is not detected. Our data further indicate that following CD38 engagement, LAT and Lck are tyrosine-phosphorylated exclusively in Brij 98-resistant rafts, and some key signaling components translocate into rafts (*i.e.* Sos and p85-phosphatidylinositol 3-kinase). Moreover, N-Ras results activated within rafts immediately upon CD38 ligation, whereas activated Erk was mainly found in soluble fractions with delayed kinetics respective to Ras activation. Furthermore, full phosphorylation of CD3-ζ and CD3-ϵ only occurs in rafts, whereas partial CD3-ζ tyrosine phosphorylation occurs exclusively in the soluble pool, which correlated with increased levels of c-Cbl tyrosine phosphorylation in the non-raft fractions. Taken together, these results suggest that, unlike the non-raft pool, CD38 in rafts is able to initiate and propagate several activating signaling pathways, possibly by facilitating critical associations within other raft subsets, for example, LAT rafts via its capacity to interact with Lck and CD3-ζ. Overall, these findings provide the first evidence that CD38 operates in two functionally distinct microdomains of the plasma membrane.

Human CD38 antigen is a 45-kDa type II transmembrane glycoprotein with a short N-terminal cytoplasmic domain and a long C-terminal extracellular domain (1, 2). It is widely expressed in different cell types including thymocytes, activated T cells, and terminally differentiated B cells (plasma cells) (3–6). Other reactive cells include NK cells, monocytes, macrophages, dendritic cells, and some epithelial cells. The CD38 antigen acts mainly as a $NAD(P)^+$ glycohydrolase (7) and plays a role in lymphocyte activation (3, 8). However, CD38 may also act as an ectocyclase that converts NAD^+ to the Ca^{2+}-releasing second messenger cyclic ADP-ribose (9). Moreover, intracellularly expressed CD38 may catalyze NAD^+/cyclic ADP-ribose conversion to cause cytosolic Ca^{2+} release (10), and CD38 may control neutrophil chemotaxis to bacterial chemoattractants through its production of cyclic ADP-ribose (11).

Plasma membranes of many cell types, including T cells, contain specialized microdomains, or lipid rafts, enriched in sphingolipids, cholesterol, sphingomyelin, and glycosylphosphatidylinositol-anchored proteins. These membrane domains are characterized by detergent insolubility at low temperatures and low buoyant density. Based on these biochemical properties, they are often referred to as glycosphingolipid-enriched membranes or detergent-insoluble glycolipid fractions (12, 13). Several signaling proteins are enriched in lipid rafts. Src family kinases and the adaptor protein LAT,[1] both of which require acylation for raft targeting, are constitutively present in rafts. The densely packed, liquid-ordered environment of rafts excludes most integral membrane proteins. However, antibody-mediated clustering can recruit receptors on several cell types to rafts. These include some components of the TCR-CD3 complex (14–17), BCR (18–20), FcϵRI (21), CD20 (22), and human CD2 (23). Other transmembrane proteins seem to be constitutively associated with rafts as CD44, CD5, CD9, and murine CD2 (24–26).

Recent data, however, demonstrate that in resting T cells 10–20% of the TCR-CD3 complex partitions into rafts that are resistant to solubilization in 1% Brij 98 at 37 °C (27), which suggests that part of the TCR-CD3 complex is constitutively associated with lipid rafts. Our previous data led to the proposition that in T cells CD38 requires the TCR-CD3 complex for signaling (28, 29). In addition, we have demonstrated that Lck,

* This work was supported in part by Instituto Carlos III-FIS, Ministerio de Sanidad y Consumo Grant 01/1073, Consejería de Salud de la Junta de Andalucía Grant 209/02 (to M. Z.), CICYT Grants SAF99-0024 and SAF2002-00721 (to J. Sancho), AIRC (Milano, Italy), TELETHON (Roma, Italy), Biotecnologia (CNR, Roma, Italy), and by the AIDS and TB projects (ISS, Rome, Italy) (to F. M.). The costs of publication of this article were defrayed in part by the payment of page charges. This article must therefore be hereby marked "*advertisement*" in accordance with 18 U.S.C. Section 1734 solely to indicate this fact.

§ Supported by Fellowship I3P from Fondo Social Europeo and Fellowship FPI from the Ministerio de Ciencia y Tecnología, Spain.

¶ Supported by Contract I3P from Fondo Social Europeo.

‖ Supported by Fellowship from CICYT Grant SAF2002-00721.

§§ Supported by a Contrato de Investigadores del Plan Nacional de Salud from the Ministerio de Sanidad y Consumo, and a contract of the program "Ramón y Cajal" from the Ministerio de Ciencia y Tecnología, Spain. To whom correspondence should be addressed: Instituto de Parasitología y Biomedicina, Consejo Superior de Investigaciones Científicas, Ventanilla, 11, 18001 Granada, Spain. Tel.: 34-958805182; Fax: 34-958203911; E-mail: mzubiaur@ipb.csic.es.

[1] The abbreviations used are: LAT, linker for activation of T cells; TCR, T cell antigen receptor; PI, phosphatidylinositol; ZAP-70, ζ-associated protein-70; Erk, extracellular signal-regulated protein kinase; Tyr(P), phosphotyrosine; mAb, monoclonal antibody; PVDF, polyvinylidene difluoride; ODG, octyl D-glucoside or *n*-octyl β-D-glucopyranoside; ECL, enhanced chemiluminescence; HRP, horseradish peroxidase; FITC, fluorescein isothiocyanate-conjugated; αmo, $F(ab')_2$ Goat anti-mouse IgG; GM1, Galβ1–3GalNacβ1–4Gal(3–2αNeuAc)β1–4Glcβ1–1-Cer; Sos, Son of Sevenless; RBD, Ras-binding domain; GST, glutathione *S*-transferase.

This is an Open Access article under the CC BY license.

which partitions into rafts, is required for CD38-mediated signaling (30), and CD38 itself is constitutively associated with lipid rafts resistant to solubilization in 1% Nonidet P-40 at 4 °C (31). Moreover, upon CD38 cross-linking, a number of proteins are tyrosine-phosphorylated including ZAP-70 and LAT (30, 31). These studies suggested that rafts and the proteins associated or targeted to them as the TCR-CD3, Lck, ZAP-70, and LAT could be involved in CD38 signaling. However, a key issue remained unclear: how is CD38 ligation coupled to activation events in rafts? Does CD38 ligation induce coalescence of membrane rafts, and does such aggregation facilitate the transactivation of the raft-associated Lck, thereby initiating the intracellular cascades, or is CD38 and a fraction of the TCR-CD3 complex constitutively present in a subset of rafts where they co-localize and physically interact?

A major concern about rafts isolated by 1% Triton X-100 or 1% Nonidet P-40 at 4 °C is that they are large vesicles of 0.5 and 1 μm in diameter, which probably results from the coalescence of segregated raft units (32). Therefore, it is difficult to interpret data on protein composition of raft subsets. However, the size of 1% Brij 98-resistant vesicles isolated at 37 °C is rather small (67 ± 39 nm) (27), which is quite close to the size (~50 nm in diameter) of circular raft patches estimated by photonic force microscopy in living fibroblasts (33) or to the size of glycosylphosphatidylinositol-anchored protein domains (less than 70 nm in diameter) measured by fluorescence resonance energy transfer microscopy in living Chinese hamster ovary cells (34). Moreover, Brij 98 vesicles are very stable, and once isolated from different cell membranes they do not coalesce (27). If a circular raft patch has a radius of about 30 nm and thus occupies 2827 nm^2, it follows that a Brij 98 vesicle on average should harbor about 1 separate raft unit, which theoretically would allow it to immunoisolate homogeneous raft subsets. Indeed, raft subsets with different protein compositions from the same membrane could actually be isolated (27).

In the present study, using 1% Brij 98 at 37 °C to isolate raft from Jurkat T cells, we have demonstrated the existence of at least three types of Brij 98-resistant raft subsets: CD38 rafts, which are enriched in CD38, CD3-ζ, and Lck; TCR/CD3 rafts, which are enriched in CD3-ζ, CD3-ϵ, and Lck; and LAT rafts, which are primarily enriched in Lck. Indeed, immunoisolated Lck rafts retrieve all the above proteins, which is in agreement with its presence in all raft subsets studied so far. Our results further indicated that following stimulation of CD38, LAT and Lck are tyrosine-phosphorylated exclusively in Brij 98-resistant rafts, and many key components of signaling pathways that are regulated by CD38 translocate into rafts (*i.e.* Sos and p85 PI 3-kinase). Moreover, N-Ras is found in its activated state within rafts upon CD38 stimulation. Furthermore, full phosphorylation of CD3-ζ and CD3-ϵ only occurs in rafts, whereas c-Cbl tyrosine phosphorylation occurs exclusively in non-raft fractions. Taken together, these data provide new insights in how rafts take part in CD38 signal transduction.

EXPERIMENTAL PROCEDURES

Cell Lines—Jurkat D8 cells, which constitutively express CD38, were obtained from wild-type Jurkat cells (subclone E6-1, American Tissue Culture Collection (ATCC), Manassas, VA) by the limiting dilution technique (35). The Lck-deficient Jurkat T cell variant JCaM1.6 (36) was kindly provided by Dr. Arthur Weiss (University of California, San Francisco).

Antibodies and Reagents—Anti-human CD3-ϵ mAb OKT3 (IgG2a) or the CD38 mAbs HB136 (IgG1) and OKT10 (IgG1) were prepared and purified by affinity chromatography on HiTrap protein A or HiTrap protein G HP column, respectively, using the ÄKTA explorer system (Amersham Biosciences) as described (28). Anti-human CD38 mAb IB4 (IgG2a) was prepared and purified by affinity chromatography on protein A-Sepharose and high pressure liquid chromatography on hydroxyapatite columns, as described (37). Anti-human CD3-ζ mAb 1D4.1 is directed against the C-terminal portion of CD3-ζ, and it has been described previously (38). Affinity-purified, fluorescein isothiocyanate-conjugated (FITC) $F(ab')_2$ fraction of rabbit antibody to mouse immunoglobulins ($F(ab')_2$ FITC-RαmIg) was purchased from Dako (Glostrup, Denmark). Affinity-purified $F(ab')_2$ fraction of goat antibody to mouse IgG (whole molecule) ($F(ab')_2$ GαmIg) was purchased from Cappel (ICN Pharmaceuticals, Inc., Costa Mesa, CA). Recombinant anti-Tyr(P) antibody coupled to horseradish peroxidase (RC20-HRP), anti-Sos1 mAb, and anti-p85 PI 3-kinase mAb were obtained from BD Biosciences. The anti-phospho-p44/42 mitogen-activated protein kinase (Thr-202/Tyr-204) E10 mouse mAb was purchased from Cell Signaling Technology (New England Biolabs, Beverly, MA). The following affinity-purified rabbit polyclonal antibodies were purchased from Santa Cruz Biotechnology (Santa Cruz, CA): anti-Erk-2, anti-ZAP-70, anti-Vav, anti-Sos, anti-Cbl, anti-p85α PI 3-kinase, and the affinity-purified mouse monoclonal antibody anti-Lck 3A5 mAb. An affinity-purified rabbit antibody to CD3-ϵ was purchased from Dako (Denmark). Polyclonal antibodies anti-LAT and anti-Lck (N-terminal) were from Upstate Biotechnology, Inc. Anti-Zap-70 (Zap-4) rabbit antiserum was a kind gift from Dr. S. C. Ley (Medical Research Council, London, UK) (30). Anti-CD3-ζ antiserum 448 was a gift from Dr. B. Alarcón (Centro de Biología Molecular, CSIC, Madrid, Spain). Affinity-purified goat anti-rabbit IgG (Fc) HRP conjugate and goat anti-mouse IgG (H+L) HRP conjugate were from Promega (Madison, WI). Prestained SDS-PAGE standards (broad and precision range), and ImmunoStart reagents were from Bio-Rad. The cholera toxin HRP-conjugated and the anti-actin mAb, AC40, were purchased from Sigma. Protein G-Sepharose 4 Fast Flow and ECL reagents were from Amersham Biosciences. Raf-1 Ras-binding domain agarose conjugate, anti-Ras (clone RAS 10, mouse monoclonal IgG2a-κ), was purchased from Upstate Biotechnology, Inc. μMACS protein G Microbeads, μMACS Separator, and μColumns were purchased from Miltenyi Biotec (Germany).

Fluorescence-activated Cell Sorter Analysis—Cells were analyzed for surface expression of CD3 and CD38 by flow cytometry as described previously by using saturating concentrations of the unlabeled primary mouse mAbs and of the $F(ab')_2$ FITC-RαmIg secondary antibody (30). Samples were analyzed in a FACScan flow cytometer (BD Biosciences), using the CellQuest Software. Under these conditions the primary antibody binds to the cell surface antigen monovalently; therefore, the number of bound antibody molecules corresponds to the number of antigenic sites (39). In experiments on peripheral blood binding of anti-CD38 mAbs tend to be exclusively monovalent when CD38 antigen density is low but partially bivalent at higher CD38 densities (40). Therefore, these estimates may be incorrect by as much as a factor of 2. However, the ratio between the median fluorescence intensities of CD3 and CD38 was constant from experiment to experiment, because the same Jurkat line was used throughout the study, and because saturating concentrations of the mAbs were used.

Detergent Solubilization of Cells at 37 °C—Cells (7–9 × 10^7) were washed twice in ice-cold RPMI/HEPES, resuspended in 0.45 ml of ice-cold 1× lysis buffer (20 mM HEPES, pH 7.6, 150 mM NaCl, 1 mM EGTA, 50 mM sodium fluoride, 1 mM sodium orthovanadate, 20 μM phenylarsine oxide, 1 mM phenylmethylsulfonyl fluoride, 10 mM iodoacetamide, and a mixture of small peptide protease inhibitors at 1 μg/ml each) without detergent to disrupt the cells (30), quick-frozen on dry ice, and then thawed on ice. Broken cells were homogenized by shearing through a 25-gauge needle with a 1-ml syringe, 10 times, on ice (41). The particulate suspension was preincubated for 4 min at 37 °C. 50 μl of a 10% Brij 98 (Sigma) stock solution in 20 mM HEPES, pH 7.4, was then added to bring a final concentration of 1% Brij 98. After 5 min of solubilization at 37 °C, the lysate was quick-frozen on dry ice and kept at −80 °C until use. Before the sucrose gradient centrifugation, lysates were thawed on ice and then diluted with 0.5 ml of lysis buffer containing 80% sucrose (final sucrose concentration 40%; final Brij 98 concentration 0.5%) and incubated on ice for 50 min (27). Samples were then placed at the bottom of a discontinuous sucrose gradient and fractionated as described below.

Fractionation of Detergent-insoluble and -soluble Fractions by Sucrose Gradient Ultracentrifugation—Detergent-insoluble and -soluble fractions were separated as described (31) with some modifications. Cell lysates were mixed with an equal volume of 80% sucrose and transferred to Sorvall ultracentrifuge tubes. Two ml of 30% sucrose, followed by 1 ml of 5% sucrose in 1× lysis buffer without detergent, were overlaid. All the sucrose solutions were prepared in 1× lysis buffer without detergent and in the presence of small peptide protease inhibitors at 1 μg/ml each, (30). Samples were centrifuged for 18–20 h at 200,000 × *g* in a Sorvall AH-650 rotor. Eight fractions of 0.5 ml each were collected on ice, from the top to the bottom of the gradients. 18-μl

aliquots of each fraction of the gradient was diluted with 9 μl of 3× Laemmli sample buffer and resolved on 12.5% SDS-PAGE under non-reducing conditions, transferred to PVDF, and immunoblotted with specific antibodies. Ganglioside GM1, which migrated with the dye front on a 12.5% SDS-PAGE gel, was detected by blotting with cholera toxin-HRP conjugated following by the ECL system.

In indicated experiments two pools of the sucrose gradient fractions were then collected. First was the low density fractions corresponding to the 5/30% interface (fractions 2 and 3, along fraction 4) and referred to as rafts. Second was the high density soluble material corresponding to fractions 7 and 8 of the gradient and referred to as soluble. Except where otherwise indicated, 18 μl of each pool were diluted with 9 μl of 3× Laemmli sample buffer and loaded onto gels. In indicated experiments proteins of each fraction of the gradient were concentrated by methanol/chloroform precipitation as described (31).

Immunoisolation of Raft Subsets under Non-solubilizing Conditions—Pooled sucrose gradient fractions 2–4 (rafts) or fractions 7–8 (soluble) were diluted with lysis buffer containing 1% Brij 98 to less than 20% sucrose. To avoid variability inherent to each sucrose gradient centrifugation, the rafts or soluble fractions from six different sucrose gradients were pooled and then divided into 6 aliquots for the immunoisolation experiments with anti-CD38, anti-Lck, anti-CD3-ζ, anti-CD3-ε, anti-LAT, or isotype-matching antibodies. After 1 h of incubation on ice with specific mAbs, 50–100 μl of protein G superparamagnetic microbeads (Miltenyi Biotec S. L. (Spain)) were added and mixed well, and the mixture was incubated for an additional 45 min on ice. Subsequently, the magnetically labeled raft subsets were passed over μColumns placed in the magnetic field of the μMACS separator following the manufacturer's specifications. The columns were then rinsed twice with 200 μl of 1% Brij 98 lysis buffer, followed 2 times by 200 μl of Solution A (0.5% Brij 98 lysis buffer), 1 time by 200 μl of Solution B (0.01% Brij 98 lysis buffer), and 1 time by 200 μl of low salt wash buffer (20 mM Tris-HCl, pH 7.5). The immunoisolated raft subsets were then eluted with 20 + 50 μl of pre-heated 95 °C hot 1× SDS gel sample buffer and the collected second eluate (50 μl) was analyzed by SDS-PAGE and Western blotting. The data shown are representative of three independent experiments.

Immunoprecipitation under Solubilizing Conditions—Pooled rafts and soluble sucrose gradient fractions were diluted with lysis buffer containing 1% Brij 98 + 60 mM ODG to less than 20% sucrose. ODG is a gentle non-ionic detergent that is very efficient in solubilizing proteins associated with rafts (42–45). Immunoprecipitation of protein assemblies was performed by incubation of these fractions with specific antibodies followed by capture of the immune complexes on protein G superparamagnetic microbeads as described above or on protein G-Sepharose 4 Fast Flow beads (Amersham Biosciences) as described elsewhere (30).

Cell Stimulation and Western Blotting—Cells were grown up to a density of 0.5–1 × 10^6/ml, centrifuged, and serum-starved in RPMI/HEPES + 0.1% fetal bovine serum 15–20 h. The cells were then washed twice in RPMI/HEPES without serum and resuspended at 4–9 × 10^7 cells per sample, or as otherwise indicated, in serum-free RPMI/HEPES medium at 4 °C. Stimulation with anti-CD38 mAbs, lysis, and Western blotting analyses were performed as described in detail elsewhere (30). Densitometric analysis was performed on a MacIntosh computer using the public domain NIH Image program version 1.62 (developed at the National Institutes of Health and available at rsb.info.nih.gov/nih-image/) or on a personal computer using the Quantity One–dimensional Analysis Software version 4.4 (Bio-Rad).

Affinity Assay for Ras Activation in Postnuclear Supernatants—D8 Jurkat T cells were grown and stimulated as described. Cells were then lysed in ice-cold 2× Mg^{2+} lysis buffer (50 mM HEPES, pH 7.5, 300 mM NaCl, 2% Igepal CA-630, 20 mM $MgCl_2$, 2 mM EDTA, 4% glycerol, 20 μg/ml aprotinin, 20 μg/ml leupeptin, 50 mM sodium fluoride, and 2 mM sodium orthovanadate) for 30 min. Postnuclear supernatants were obtained by centrifugation at 13,000 × *g* for 15 min at 4 °C. Activated Ras was assayed on equivalent amounts of lysates from unstimulated or anti-CD38-stimulated cells. The lysates were incubated with GST-Raf1-RBD (Ras-binding domain) as specified by the manufacturer (Upstate Biotechnology, Lake Placid, NY). Proteins were eluted with 3× Laemmli reduced sample buffer and applied to either a 12.5 or a 15% SDS-PAGE under reducing conditions. Proteins were transferred to a PVDF membrane, blocked at room temperature for 1 h in 5% milk, and probed with anti-Ras antibody overnight at 4 °C (clone RAS 10) (46). Total Ras was measured by anti-Ras immunoblot analysis of an aliquot of the postnuclear lysate followed by an HRP-conjugated anti-mouse secondary. Proteins were detected using enhanced chemiluminescence (ECL System, Amersham Biosciences, or ImmunoStart System from Bio-Rad).

Affinity Assay for Ras Activation in Raft and Soluble Fractions—Pooled raft and soluble fractions from 4 to 5 × 10^6 unstimulated or anti-CD38-stimulated Jurkat T cells were diluted with 1× Mg^{2+} lysis buffer to bring the sucrose concentration to less than 20%. Samples were then incubated with GST-RBD and processed as above.

Statistical Analysis—Statistical analysis were performed using the Student's *t* test parametric) to compare sample groups. *p* values less than 0.05 were considered significant.

RESULTS

Isolation and Characterization of CD38-containing Brij 98-insoluble Raft Microdomains—In this study we used Jurkat T cells, which constitutively express CD38 (30) (Fig. 1*A*), to test whether CD38-mediated signaling is initiated within rafts. We first investigated whether CD38 is associated with the membrane raft vesicles that are recovered as detergent-insoluble complexes upon solubilization of cells in Brij 98 at 37 °C. This detergent has a hydrophilic-lipophilic balance of 15.3 mM, and it has been successfully used to selectively isolate detergent-insoluble microdomains at 37 °C exhibiting the expected biochemical characteristics of rafts (27). Jurkat T cells were lysed in 1% Brij 98 at 37 °C as described under "Experimental Procedures," and the lysates were fractionated into supernatant and pellet after centrifugation at 13,000 × *g* for 15 min. As shown in Fig. 1*B*, only about 42% of CD38 was found in the supernatant (*lane 1*), and therefore, most CD38 was found precipitated in the pellet (*lane 3*). These results demonstrated that a large fraction of CD38 was insoluble in Brij 98 at 37 °C and strongly suggested that CD38 was associated with Brij 98-resistant lipid rafts. However, insolubility of a membrane protein in a non-ionic detergent could be due to its association with detergent-resistant lipid rafts and/or its anchoring to cytoskeletal elements. To distinguish between these two possibilities, we used ODG, which is a gentle non-ionic detergent that is very efficient in solubilizing proteins associated with glycolipid-enriched membranes, and it does not disrupt the cytoskeleton (42–45). As shown in Fig. 1*B, lane 2*, in cells lysed in 1% Brij 98 in the presence of 60 mM ODG about 98% of CD38 was recovered in the supernatant upon centrifugation at 13,000 × *g* for 15 min, which indicated that CD38 was almost entirely solubilized by ODG. Therefore, the efficiency of ODG to solubilize CD38 supports the conclusion that its insolubility in Brij 98 is due to raft association and not to cytoskeleton interactions.

To confirm this, raft membranes were isolated from Jurkat T cells by using a flotation assay based on resistance to solubilization by Brij 98 at 37 °C (27), and buoyancy at low density fractions of a bottom-loaded discontinuous sucrose gradient, with steps of 5, 30, and 40% sucrose (31). As shown in Fig. 1*C*, most of the transmembrane proteins CD38 and LAT, the intracellular membrane-bound Lck, and the ganglioside GM1 partitioned into low density fractions 2–4, which is consistent with its residency in floating lipid rafts or glycolipid-enriched membranes. Thus, densitometric analysis showed that the CD38 present in rafts was composed of 62.2 ± 3.7% of the total CD38, whereas the CD38 present in soluble fractions 7–8 was 35.0 ± 3.9% of total CD38 ($p < 0.006$, $n = 10$, Table I). Likewise, 73.9 ± 4.7% of total GM1 localized to rafts, whereas only 13.1 ± 2.5% was in soluble fractions ($p < 0.00001$, $n = 10$, Table I). Moreover, about 84% of Lck, 75% of LAT, and less than 30% of CD3-ζ and CD3-ε were enriched in floating rafts. In contrast, about 10% of ZAP-70 and none of actin or Cbl were detected in those fractions (Fig. 1*C*, and data not shown). These low density fractions contained only about 2% of total proteins found in the whole sucrose gradient (Fig. 1*D*); therefore they were highly enriched in proteins associated with lipid rafts.

We next examined how ODG affected the recovery of CD38, CD3-ζ, CD3-ε, LAT, Lck, and the ganglioside GM1 in floating

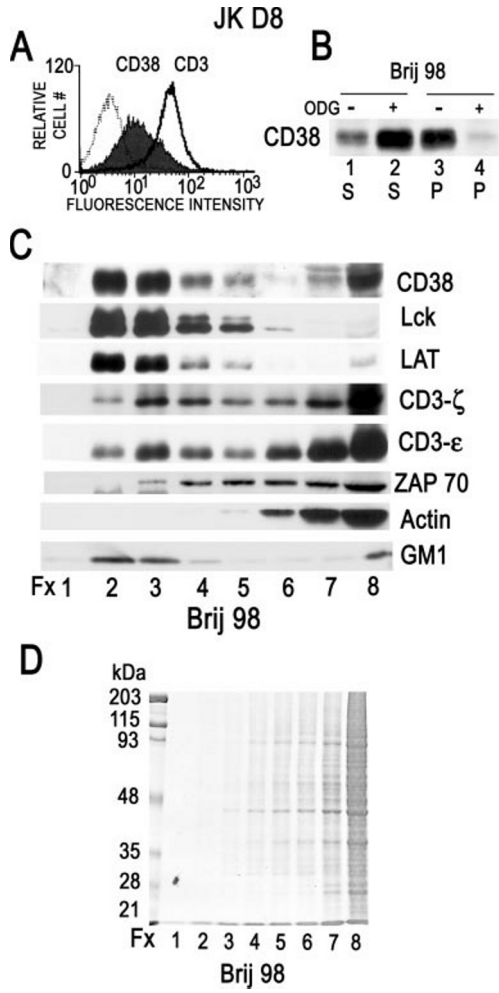

FIG. 1. **Isolation and characterization of CD38-containing detergent-insoluble membrane microdomains using Brij 98 at 37 °C.** *A*, the surface expression of CD3 and CD38 was analyzed by indirect immunofluorescence staining with saturating concentrations of both primary and secondary antibodies. Thus, Jurkat D8 cells were incubated with the anti-human CD3-ϵ mAb OKT3 (*open histogram*, *continuous line*) or with the anti-human CD38 mAb HB136 mAb (*filled histogram*), followed by incubation with $F(ab')_2$ FITC-anti-mouse IgG secondary antibody. Representative flow cytometric profiles are shown. Negative controls were obtained after staining with an isotype-matching unrelated mAb plus a secondary antibody (*open histogram*, *dotted line*). Flow cytometric data are presented as the logarithm of fluorescence intensity. Median fluorescence intensity after subtraction of the fluorescence detected with an isotype-matched control was 38.02 and 7.74 for CD3 and CD38, respectively. The data shown are representative of more than 20 independent experiments. *B*, Jurkat T cells were lysed in 1% Brij 98-containing lysis buffer at 37 °C for 5 min (−) or with 1% Brij 98 in the presence of 60 mM ODG (+). Cell lysates were fractionated into a supernatant of soluble proteins (*S*) and a pellet (*P*) of insoluble proteins by centrifugation at 13,000 × *g* for 15 min at 4 °C, as described under "Experimental Procedures." Proteins were separated on 11% SDS-PAGE under non-reducing conditions, and upon transference to PVDF membranes were immunoblotted with the anti-CD38 mAb HB136. Blot in *B* was scanned, and CD38 bands were quantified using the NIH Image program 1.62 version. CD38 in either the supernatant or in the pellet was expressed as percentage of total (sum of supernatant plus pellet). The numbers are as follows: 42% (*lane 1*), 98% (*lane 2*), 58% (*lane 3*), and 2% (*lane 4*). The data shown are representative of three independent experiments. *C*, Jurkat T cells were lysed in 1% Brij 98-containing lysis buffer at 37 °C for 5 min and fractionated on a sucrose gradient as described under "Experimental Procedures." Eight fractions of 0.5 ml were collected from the top to the bottom of the gradient. 18-μl aliquots of each fraction of the gradient were diluted with 9 μl of 3× Laemmli non-reducing sample buffer, and the resulting 27 μl were resolved on 12.5% SDS-PAGE under non-reducing conditions, transferred to PVDF, and blotted with specific antibodies against the indicated proteins to the *right of each panel*. Ganglioside GM1, which migrated with the dye front of the 12.5% SDS-PAGE gel, was detected by blotting with cholera toxin-HRP conjugated by following the ECL system. A representative experiment is shown from more than 10 independent experiments. Blots in *C* were scanned, and protein bands were quantified using the NIH Image program 1.62 version. The percentage of each protein that migrated to low and high density fractions is shown in Table I. *D*, an 18-μl aliquot of each gradient fraction was resolved on SDS-PAGE as above and stained with Coomassie Blue. The gel was scanned and protein bands were quantified using the NIH Image version 1.62 software system. A representative experiment is shown from five independent experiments. The results were confirmed by analyzing the same fractions in solution with the Bio-Rad colorimetric protein assay (data not shown).

rafts by treating the Brij 98 lysates with 60 mM ODG before gradient centrifugation. As shown in Table I, ODG dissociated >50% of CD38, LAT, and GM1 from the top fractions, whereas Lck was less affected (about 28% of Lck moved out of the raft fractions). Note, however, that only 43% of CD38 migrated to high density fractions 7–8 upon ODG treatment, despite the fact that same treatment yielded little pelletable CD38 upon centrifugation at 13,000 × *g* (Fig. 1*B*). Likewise, ODG seemed not to affect the recovery of CD3-ζ or CD3-ϵ in the low density fractions, although there was a small but highly reproducible reduction in the percentage of these proteins found in the high density fractions 7–8 (Table I). These apparent contradictions were caused by the appearance in fractions 5–6 of CD38, CD3-ζ, and CD3-ϵ forms of greater buoyant density than those floating to fractions 2–4 but with lower densities than those remaining in fractions 7–8 (data not shown). These data suggest that ODG caused partial solubilization with the appearance of less buoyant CD38, CD3-ζ, and CD3-ϵ complexed with sphingolipid and other lipids in non-vesicular form (47), or forming vesicles of smaller size (nanovesicles) with a distinct cholesterol/lipid environment than that in fractions 2–4 (48). Therefore, ODG altered the buoyant properties of CD38, CD3-ζ, and CD3-ϵ shifting to intermediate densities.

Lck and the TCR-CD3 Complexes Are Specifically Concentrated in Anti-CD38 Immunoisolated Rafts—We next examined whether the CD3 subunits and Lck are located within the same raft subset as CD38. To this end, CD38-containing rafts were immunoisolated from the total pool of Brij 98-resistant raft fractions with μMACS protein G Microbeads as described under "Experimental Procedures." Then the immunoisolated rafts bound to the anti-CD38-coated magnetic beads were analyzed biochemically. Western blot analysis showed that nonspecific binding of CD38 to an irrelevant isotype-matching mouse mAb (IgG1) was about 1% of the total amount of CD38 in the pooled raft fractions 2–4, whereas its specific binding to the anti-CD38 mAb OKT10 was about 38%, which suggested a substantial enrichment over the amount in the pooled raft fraction (data not shown), despite the fact that these experiments were done in antigen excess according to the manufacturer's specifications. Similar analysis showed that Lck, CD3-ζ, CD3-ϵ, and LAT were also detected in rafts immunoisolated with the anti-CD38 mAb, OKT10 (Fig. 2*A*, *lane 1*), although there was a hierarchy of binding, Lck > CD3-ζ ≫ CD3-ϵ ≥ LAT. Binding of CD3-ϵ and LAT to OKT10 was considered nonspecific because it was in the range of that bound to the irrelevant isotype-matching mAb (0.2–0.8%). Then, we examined the protein composition of the rafts immunoisolated with anti-Lck, anti-CD3-ζ, anti-CD3-ϵ, or anti-LAT antibodies. The data showed that Lck, CD38, and CD3-ζ were readily detected in rafts immunoisolated with the anti-Lck mAb 3A5 (Fig. 2*A*, *lane 2*). Likewise, CD3-ζ, CD38, and Lck were clearly present in rafts immunoisolated with the anti-CD3-ζ mAb 1D4.1 (Fig. 2*A*, *lane 3*). Moreover, significantly higher amounts of LAT were detected in Lck- than in CD3-ζ-immunoisolated rafts (Fig. 2*A*, *lanes 2* and *3,* respectively). Regarding CD3-ϵ rafts immunoiso-

TABLE I

Effects of detergents Brij 98 or ODG on the floatability of cell surface and intracellular membrane-associated molecules

Jurkat T cells were lysed in 1% Brij 98 or in 1% Brij 98 + 60 mM ODG before sucrose gradient centrifugation as described under "Experimental Procedures." 0.5-ml fractions were collected, and aliquots of each fraction were analyzed by Western blot for the indicated proteins or ganglioside GM1. Densitometric data on rafts (fractions 2–4) and soluble (fractions 7–8) pools are presented as percentage of the sum of all sucrose gradient fractions (fractions 1–8).

	Rafts		Soluble	
	Brij 98	Brij 98 + ODG	Brij 98	Brij 98 + ODG
CD38	62.2 ± 3.7[a]	28.7 ± 0.2[b]	35.0 ± 3.9[a]	43.2 ± 1.7[b]
Lck	83.7 ± 4.0[c]	59.8 ± 9.4[b]	6.2 ± 3.2[c]	20.7 ± 14.4[b]
LAT	75.1 ± 13.6[c]	25.5 ± 5.0[b]	20.3 ± 11.4[c]	54.3 ± 2.0[b]
CD3-ζ	22.6 ± 2.0[c]	23.4 ± 2.4[b]	61.9 ± 1.4[c]	49.9 ± 2.1[b]
CD3-ε	26.8 ± 6.5[c]	31.3 ± 6.4[b]	54.6 ± 7.8[c]	40.5 ± 6.1[b]
GM1	73.9 ± 4.7[a]	36.6 ± 3.2[b]	13.1 ± 2.5[a]	37.3 ± 5.7[b]

[a] The data are the means ± S.E. of 10 independent experiments.
[b] The data are the means ± S.E. of 2 independent experiments.
[c] The data are the means ± S.E. of 3 independent experiments.

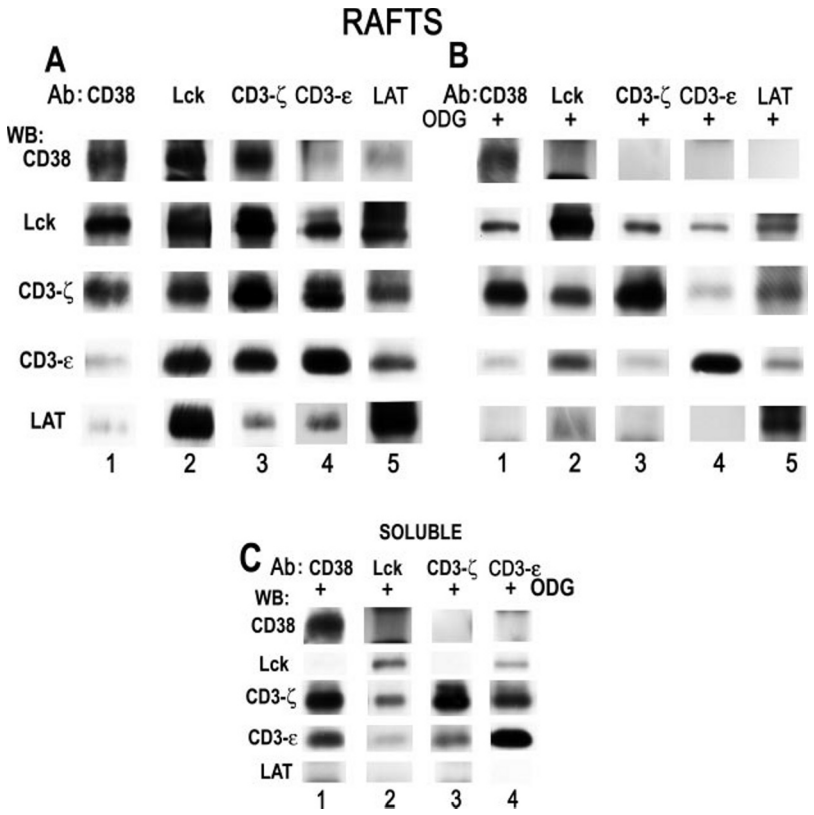

FIG. 2. **Lck and CD3-ζ are associated with CD38 in membrane rafts.** *A*, Jurkat T cells were lysed in 1% Brij 98 at 37 °C for 5 min. Rafts were isolated by sucrose gradient ultracentrifugation, and pooled fractions 2–4 were resuspended in 1% Brij 98 lysis buffer. The raft subsets enriched in CD38 (*lane 1*), Lck (*lane 2*), CD3-ζ (*lane 3*), CD3-ϵ (*lane 4*), or LAT (*lane 5*) were immunoisolated with specific antibodies (*Ab*) and μMACS protein G microbeads as described under "Experimental Procedures." Immunoisolates were separated on 11% SDS-PAGE gels under non-reducing conditions and blotted with the indicated antibodies. The amount of CD38, Lck, CD3-ζ, CD3-ϵ, or LAT in the corresponding immunoisolates was estimated by comparison with the total amount of each protein recovered in the pooled raft fractions 2–3, and ranged from 22% for Lck up to 51% for CD3-ϵ. Nonspecific binding to an isotype-matched mouse immunoglobulin (IgG1) ranged from 0.1 to 1%. *WB*, Western blot. *B*, pooled raft fractions isolated as in *A* were prepared and treated for raft solubilization with 1% Brij 98 + 60 mM ODG lysis buffer before being subjected to immunoprecipitation with anti-CD38 (*lane 1*), anti-Lck (*lane 2*), anti-CD3-ζ (*lane 3*), anti-CD3-ϵ (*lane 4*), or anti-LAT (*lane 5*) mAbs bound to μMACS protein G microbeads. Immunoprecipitates were blotted with the indicated antibodies. *C*, soluble fractions were prepared and treated as in *B* with 1% Brij 98 + 60 mM ODG before being subjected to immunoprecipitation with anti-CD38 (*lane 1*), anti-Lck (*lane 2*), anti-CD3-ζ (*lane 3*), or anti-CD3-ϵ (*lane 4*) mAbs bound to μMACS protein G microbeads. Immunoprecipitates were blotted with the indicated antibodies. The data shown are representative of at least three independent experiments.

lated with the anti-CD3-ϵ mAb OKT3, CD3-ζ was the major protein co-isolated, following by Lck, with relatively weaker detection of LAT and CD38 (Fig. 2*A*, *lane 4*). This correlated with the fact that CD3-ϵ was readily detected in both Lck- and CD3-ζ-immunoisolated rafts (Fig. 2*A*, *lanes 2* and *3*) showed intermediate levels in LAT rafts and was weakly detected in CD38-immunoisolated ones (Fig. 2*A*, *lanes 1* and *5*, respectively).

The higher level of Lck relative to LAT in CD3-ζ- and CD3-ϵ-immunoisolated rafts indicated that TCR-CD3 raft distribution in Jurkat T cells was very similar to that in the murine T cell line 3A9 lysed in Brij 98 (27). Of note is that LAT was readily detected in Lck rafts and vice versa Lck was clearly present in LAT rafts, whereas the amount of the other proteins was significantly higher in Lck rafts than in LAT rafts (Fig. 2*A*, *lanes 2* and *5*), which is in agreement with the strong presence of Lck in all raft subsets studied so far and suggesting that Lck is the linker that keeps most of these proteins together.

ODG Extraction Reveals Distinct Protein Assemblies within Rafts, Which Differ in Their Requirements for Stable Association—To examine whether the protein assemblies detected in immunoisolated rafts correspond to protein-protein interactions or whether they are dependent on the raft integrity, pooled low density Brij 98-resistant raft vesicles were resuspended in a buffer containing 1% Brij 98 + 60 mM ODG, which efficiently disrupts many lipid raft-protein associations (see Table I). Then either CD38, Lck, CD3-ζ, CD3-ϵ, or LAT was immunoprecipitated with specific antibodies bound to μMACS protein G microbeads as described above, and the retrieved proteins were detected by Western blot analysis (Fig. 2*B*). Because ODG did not affect much the interaction of Lck with lipid rafts, although greatly affecting the CD38-raft interaction (Table I), it was expected that in ODG-treated raft vesicles the ratio Lck/CD38 would be significantly higher than that in Brij 98-resistant ones. In this sense, CD38 was no longer detectable in the Lck immunoprecipitates from ODG-treated raft vesicles (Fig. 2*B*, *lane 2*), whereas Lck was still detectable in the CD38 immunoprecipitates (Fig. 2*B*, *lane 1*). Note, however, that the relative amount of Lck co-immunoprecipitated with CD38 was significantly reduced as compared with that in the intact raft vesicles (Fig. 2, *B* and *A*, *lane 1*). These data were in accordance with the reduced amount of CD38 that still remained associated with raft fractions upon ODG treatment (Table I) and therefore susceptible to interact with Lck, or being part of the same raft subset. Likewise, in the presence of ODG LAT was no longer detected in CD3-ζ or CD3-ϵ immunoprecipitates (Fig. 2*B*, *lanes 3* and *4*, respectively), and vice versa, low amounts of CD3-ζ and CD3-ϵ were co-immunoprecipitated with LAT (Fig. 2*B*, *lane 5*). Again, these data correlated with the ability of ODG to selectively disrupt raft-LAT association, whereas the association of either CD3-ζ or CD3-ϵ with lipid rafts was less affected (Table I).

Other protein assemblies were affected by the presence of ODG but not completely disrupted. Thus, lower amounts of LAT was co-immunoprecipitated with Lck as compared with that in Brij 98 alone (Fig. 2, *B versus A*, *lane 2*), and vice versa a lower amount of Lck was detected in LAT immunoprecipitates than that in Brij 98 (Fig. 2, *B versus A*, *lane 5*), which is in agreement with a recent report (49) showing that in Jurkat cells solubilized in 1% Triton X-100 LAT preferentially interacts with the open active form of Lck and weakly with the closed non-active Lck in lipid rafts, the latter being the predominant form in unstimulated Jurkat cells.

On the other hand, in the presence of ODG the associations of Lck with CD3-ζ or with CD3-ϵ were readily detectable, although the relative amounts of CD3-ζ and CD3-ϵ co-immunoprecipitated with Lck were significantly reduced (Fig. 2*B*, *lane 2*) as compared with that in Brij 98 alone (Fig. 2*A, lane 2*). Moreover, CD3-ζ-Lck and CD3-ϵ-Lck interactions were detectable despite much less Lck was co-immunoprecipitated with both CD3 subunits (Fig. 2, *B versus A*, *lanes 3* and *4*).

CD38 Associates with CD3-ζ in Both Raft and Soluble Fractions—Because both the TCR-CD3 complex and CD38 were present in raft and soluble fractions, it was of interest to know whether they could interact in both compartments. The data clearly showed that the presence of ODG did not significantly affect the amount of CD3-ζ co-immunoprecipitated with CD38 in low density fractions (Fig. 2*B*, *lane 1*) as compared with that retrieved in Brij 98-resistant CD38-containing raft vesicles (Fig. 2*A*, *lane 1*). Moreover, CD3-ζ was readily detected in CD38 immunoprecipitates from the non-raft fraction either in the presence of ODG (Fig. 2*C*, *lane 1*) or in Brij 98 alone (data not shown). It is worth noting that although CD3-ϵ was also detected in the CD38 immunoprecipitates from soluble fractions

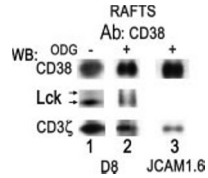

FIG. 3. **CD38 is associated with CD3-ζ in the absence of Lck.** Pooled raft fractions from sucrose gradient from Brij 98 lysates from Jurkat D8 (*lanes 1 and 2*) or JCaM 1.6 cells (*lane 3*) were immunoprecipitated with the anti-CD38 mAb OKT10 in the presence of 1% Brij 98 alone (*lane 1*) or in the presence of 1% Brij 98 + 60 mM ODG (*lanes 2* and *3*) using protein G-bound-Sepharose beads as described previously (30). Immunoprecipitates were separated on 11% SDS-PAGE gels under non-reducing conditions and blotted with the indicated antibodies to the *left of each panel*. The data shown are representative of at least three independent experiments. *WB*, Western blot.

(Fig. 2*C, lane 1*), its concentration in CD38 raft fractions was significantly lower than that of CD3-ζ (Fig. 2, *A* and *B*, *lane 1*), which suggested that, at least in rafts, CD38-CD3-ζ interaction could occur independently of the presence of the other subunits of the TCR-CD3 complex or at other CD3-ζ/CD3-ϵ ratios than that of the TCR-CD3 complex. Moreover, CD38-CD3-ζ association also occurred in soluble fractions were Lck did not co-immunoprecipitate with CD38 (Fig. 2*C*, *lane 1*), and in ODG-solubilized rafts from the Lck-deficient Jurkat variant JCaM 1.6 (Fig. 3, *lane 3*), which strongly suggests that Lck is not required for CD38-CD3-ζ interaction. Together, these results emphasize that the association of CD38 with CD3-ζ can occur outside of raft membrane vesicles and that CD38-CD3-ζ complexes are not artifacts of incomplete solubilization but instead represent discrete units that are capable of being fully solubilized.

However, CD38 was not detected in CD3-ζ immunoprecipitates from either ODG-solubilized rafts or non-raft compartments (Fig. 2, *B* and *C*, *lane 3*), which was a clear discrepancy from the data in intact raft vesicles where CD38 is readily retrieved by CD3-ζ immunoisolates (Fig. 2*A*, *lane 3*), and suggested an interaction of either low affinity or low stoichiometry. Against the low affinity of the CD38-CD3-ζ interaction is the fact that upon extraction with ODG, CD3-ζ is still readily detectable in CD38 immunoprecipitates (Fig. 2*B*, *lane 1*, and Fig. 3, *lane 2*), while almost undetectable in the CD3-ϵ immunoprecipitates (Fig. 2*B*, *lane 4*). Likewise, relatively lower amounts of CD3-ϵ were co-immunoprecipitated with CD3-ζ in the ODG-treated raft compartment (Fig. 2*B*, *lane 3*), as compared with those in Brij 98 alone (Fig. 2*A*, *lane 3*), which suggests that CD38-CD3-ζ interaction has a relatively higher affinity than that of the well established CD3-ϵ-CD3-ζ association (50).

Moreover, it is worth noting that in Jurkat T cells TCR-CD3 surface expression was significantly higher than that of CD38, with a CD3/CD38 ratio of about 5:1 at saturating concentrations of both the anti-CD3-ϵ and anti-CD38 mAbs (Fig. 1*A*), which is indicative of a higher number of surface CD3 molecules than that of CD38. However, because these proteins are not equally distributed in the different cell surface microdomains, the real number of CD3 and CD38 molecules in each microdomain may vary significantly. One might expect that in Brij 98-resistant rafts CD38 and CD3-ζ will be constrained to be close together at a more balanced concentration, and hence they were readily co-isolated independently of the antibody used for immunoisolation (Fig. 2*A*, *lanes 1* and *3*). In contrast, in Brij 98- or ODG-soluble fractions the number of CD3 molecules clearly exceeds those of CD38; therefore, it is expected that a large proportion of CD3-ζ will be associated with receptors other than CD38 (*i.e.* the TCR-CD3 complex), or it will be remain free. Under conditions of large antigen excess, as occurs

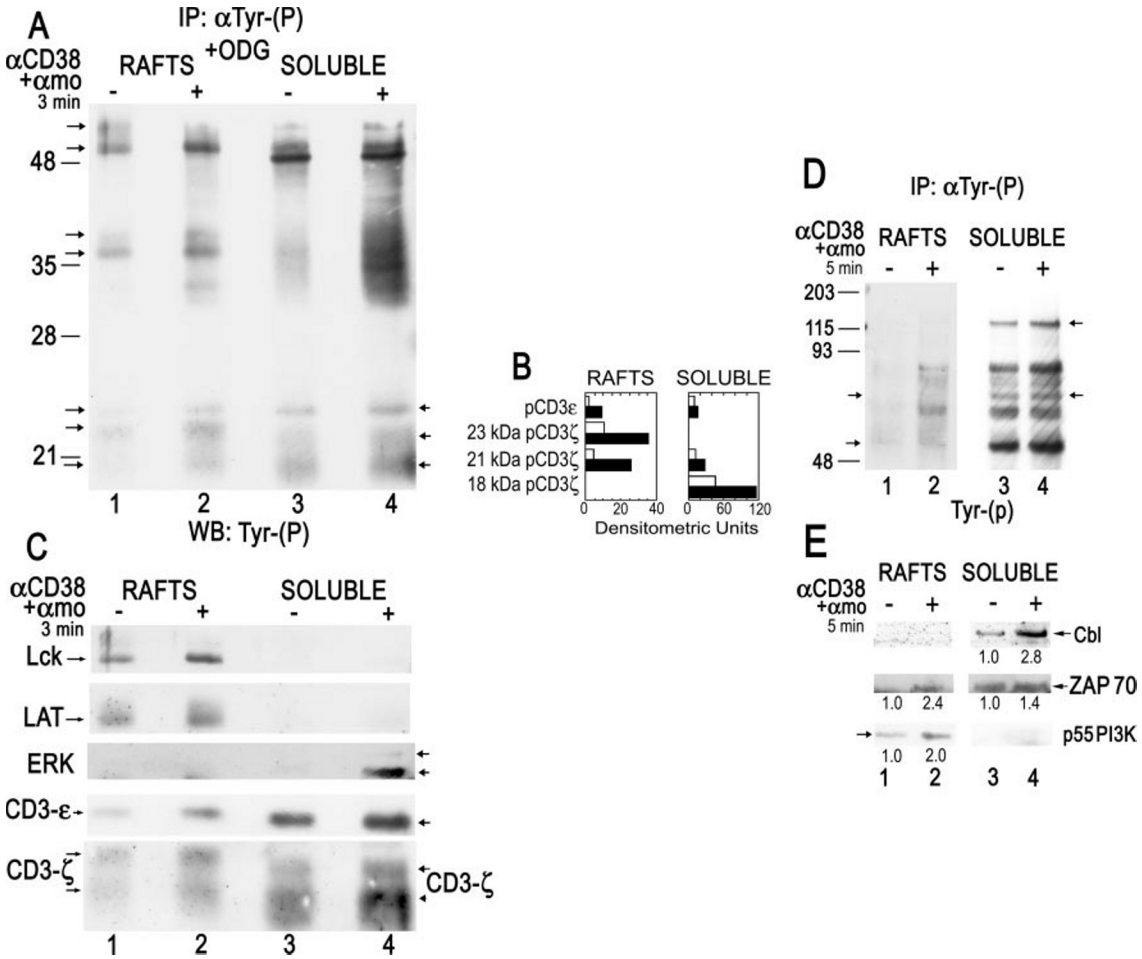

FIG. 4. **Upon CD38 engagement LAT, Lck, CD3-ζ, and CD3-ε tyrosine phosphorylation occurs in rafts, whereas c-Cbl tyrosine phosphorylation occurs in non-raft soluble fractions.** *A*, serum-starved Jurkat D8 T cells were stimulated (+) or not (−) with the anti-CD38 mAb IB4 at 5 μg/10^7 cells, followed by cross-linking with the $F(ab')_2$ fragment of a secondary antibody for 3 min at 37 °C. Cells were then lysed in 1% Brij 98 at 37 °C, and rafts and soluble fractions were isolated by sucrose gradient centrifugation as described under "Experimental Procedures." 60 mM ODG + 1% Brij 98-containing lysis buffer was then added to these fractions, and they were subjected to immunoprecipitation (*IP*) with an anti-Tyr-(P) mAb bound to agarose beads. Tyrosine-phosphorylated proteins were eluted from the beads with 40 mM phenyl phosphate. Proteins were separated on 11% SDS-PAGE under reducing conditions and blotted with the anti-Tyr(P) mAb RC20-HRP. The position of molecular mass markers is indicated to the *left*. *B*, blots in *A* were scanned, and tyrosine-phosphorylated CD3-ε and CD3-ζ bands were quantified using the NIH Image program 1.62 version. *Open bars* represent the amount of each phosphoprotein expressed in densitometric units before stimulation. *Closed bars* represent that upon IB4 stimulation. *C*, filter from *A* was subsequently stripped and reprobed with specific antibodies against the indicated proteins. The data shown are representative of three independent experiments. *D*, Jurkat T cells were stimulated (+) or not (−) with IB4+αmo for 5 min at 37 °C. Then rafts and soluble fractions were isolated. Tyrosine-phosphorylated proteins were immunoprecipitated and immunoblotted with anti-Tyr(P) mAb as above, except that 1% Brij 98-containing lysis buffer without ODG was added before the immunoprecipitation. The position of molecular mass markers is indicated to the *left*. *E*, filter from *D* was stripped and reprobed with antibodies against the indicated proteins. Fold increase in the densitometric units (corrected by area) relative to unstimulated cells is indicated at the *bottom of each lane*. The data are representative of three independent experiments.

in our immunoprecipitation experiments, it is likely that the anti-CD3-ζ mAb would bind much more the CD3-ζ molecules that remain free or associated with other receptors (Fig. 2, *B* and *C*, *lane 3*), rather than associated with CD38, which would be preferentially captured by the anti-CD38 mAb (Fig. 2, *B* and *C*, *lane 1*). Therefore, these findings support the idea that the CD38 raft subset represents a significant fraction of CD3-ζ-containing rafts, whereas CD38 in the disordered plasma membrane represents a very minor fraction of CD3-ζ-associated complexes.

Tyrosine Phosphorylation of Lck, LAT, and Fully Phosphorylation of CD3-ζ and CD3-ε Occurs Exclusively in Rafts upon CD38 Engagement—The first signaling events following CD38 engagement involve increased tyrosine phosphorylation of a number of cellular proteins, including ZAP-70, Lck, LAT, and the CD3 subunits, CD3-ζ and CD3-ε (28, 30, 31). To analyze whether these events occur in rafts, pooled Brij 98-resistant raft and soluble fractions from unstimulated or IB4-stimulated cells were treated with 1% Brij 98 + 60 mM ODG before immunoprecipitation with an anti-Tyr(P) mAb bound to agarose beads. This was followed by elution of tyrosine-phosphorylated proteins with 40 mM phenyl phosphate, Western blot with anti-Tyr(P) mAb, and subsequent re-blotting with specific antibodies as described (30). As shown in Fig. 4, *A* and *C*, Lck and LAT were readily detected in the anti-Tyr(P) immunoprecipitates from rafts with a significant increase upon CD38 ligation for 3 min (in Fig. 4*C*, compare *lane 1* with *lane 2*). Neither Lck nor LAT was detected in the anti-Tyr(P) immunoprecipitates from the soluble fraction (Fig. 4, *A*, and *C*, *lanes 3* and *4*). In contrast, tyrosine-phosphorylated Erk was mainly detected in the soluble fraction (*lane 4*). Tyrosine phosphorylation of Erk correlates with increased Erk catalytic activity (30).

Tyrosine phosphorylation of CD3-ε and CD3-ζ occurred in both raft and soluble fractions upon CD38 ligation (Fig. 4, *A* and *C*). However, in rafts CD3-ε tyrosine phosphorylation increased 4-fold relative to that in unstimulated cells, whereas in

the soluble fraction such an increase was only 1.7-fold (for quantification see Fig. 4*B*). Likewise, the increases in CD3-ζ tyrosine phosphorylation were more prominent in rafts than in soluble fractions (3–5-fold in rafts *versus* 2-fold in soluble fractions, Fig. 4*B*). It is worth noting that in the raft fraction tyrosine-phosphorylated CD3-ϵ exhibited a slower migration on SDS-PAGE than its counterpart in the soluble fraction (Fig. 4, *A* and *C*, *lanes 1* and *2 versus lanes 3* and *4*). Its apparent molecular weight coincided with that of the upper band of the fully tyrosine-phosphorylated CD3-ϵ, which runs as a 24–25-kDa doublet on high resolution SDS-PAGE (38). Likewise, the 23-kDa form of tyrosine-phosphorylated CD3-ζ, which corresponds to that of fully phosphorylated CD3-ζ species (51), was only detected in rafts and not in the soluble fraction. In contrast, in the soluble fraction from IB4-stimulated cells 81% of tyrosine-phosphorylated CD3-ζ migrated with an apparent molecular mass of 18 kDa (Fig. 4, *A*, *lane 4*, and *B*). Moreover, in rafts from IB4-stimulated cells the 23-kDa form was predominant over the 21-kDa form (Fig. 4, *A*, *lane 2*, and *B*). Both the 21- and 18-kDa forms correspond to partially phosphorylated CD3-ζ species (51). The appearance of fully phosphorylated CD3-ζ and a 23:21-kDa ratio near 1 has been correlated with the activation of ZAP-70 and T cell activation, whereas altered CD3-ζ phosphorylation and a 23:21 ratio of much less than 1 has been associated with partial TCR signaling (51–54).

c-Cbl Tyrosine Phosphorylation Occurs Exclusively in the Soluble Fraction upon CD38 Engagement—c-Cbl is a cytosolic protein that becomes tyrosine-phosphorylated upon CD38 engagement although with slower kinetics than those of LAT, CD3-ϵ, and CD3-ζ (28, 30). Because in Jurkat T cells anti-CD3 stimulation induces the association of a highly tyrosine-phosphorylated pool of c-Cbl with lymphocyte membranes and with a detergent-insoluble particulate fraction (55), it was of interest to examine whether this phenomenon occurred upon CD38 ligation. To this end, cells were stimulated for 5 min with the anti-CD38 mAb IB4 followed by cross-linking with the $F(ab')_2$ fraction of a secondary antibody. Then pooled Brij 98-resistant raft and soluble sucrose gradient fractions from unstimulated or IB4-stimulated cells were immunoprecipitated with an anti-Tyr(P) mAb bound to agarose beads as described above. As shown in Fig. 4*E*, c-Cbl was exclusively detected in the anti-Tyr(P) immunoprecipitates from the soluble fraction, with a significant increase upon CD38 engagement (Fig. 4*E*, *upper panel*, *lanes 3* and *4*). In contrast, tyrosine phosphorylation of p55 PI 3-kinase was exclusively detected in raft fractions (Fig. 4*E*, *lower panel*, *lanes 1* and *2*), whereas phospho-ZAP-70 was detected in both raft and soluble fractions, although after CD38 stimulation the increase in ZAP-70 tyrosine phosphorylation was seen better in the raft fraction (Fig. 4*E*, *middle panel*). Increased ZAP-70 tyrosine phosphorylation has been correlated with augmentation of its catalytic activity (56), whereas c-Cbl has been associated with the negative regulation of immune receptor signaling (57). Note that in both raft and soluble fraction from cells stimulated with anti-CD38 mAb for 5 min, several tyrosine-phosphorylated proteins were detected, with apparent molecular masses above 50 kDa. However, in the soluble fraction the relative abundance of tyrosine-phosphorylated proteins was higher than in rafts, which correlated with its higher protein content. Overall, these findings strongly corroborate our initial suggestion that raft microdomains play an important role in the activation of the earliest CD38 signaling events (31), in which Lck, CD3-ζ, CD3-ϵ, ZAP-70, and LAT become tyrosine-phosphorylated. In contrast, potentially inhibitory signals involving altered CD3-ζ tyrosine phosphorylation and fully c-Cbl tyrosine phosphorylation could be initiated simultaneously, or a few minutes later in the bulk of non-raft plasma membrane and/or the cytosol.

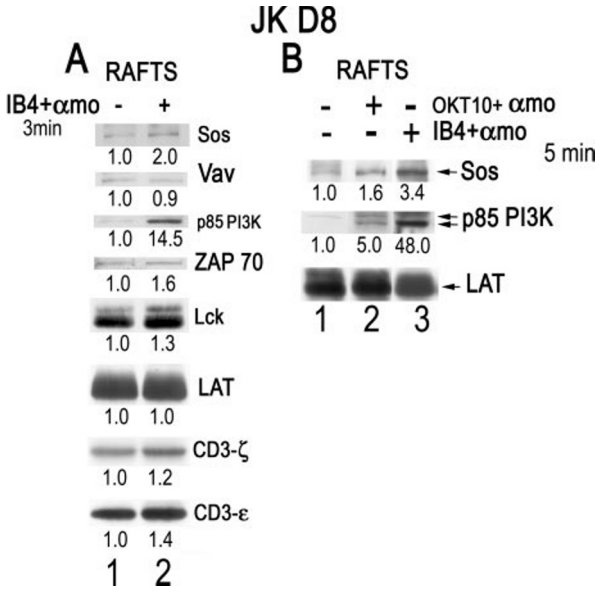

FIG. 5. **Recruitment of Sos and p85 PI 3-kinase to membrane rafts upon CD38 ligation.** *A*, overnight serum-starved Jurkat T cells (*JK D8*) were left unstimulated (−) or they were stimulated (+) with the anti-CD38 mAb antibody IB4 (5 μg/10^7 cells), followed by cross-linking with the $F(ab')_2$ fragment of a secondary antibody (*αmo*) for 3 min at 37 °C. Cells were then lysed in 1% Brij 98-containing lysis buffer at 37 °C for 5 min. Rafts were isolated and concentrated as described under "Experimental Procedures." 25-μl aliquots (in sample buffer) of rafts fractions were resolved on 11% SDS-PAGE under non-reducing conditions and transferred to PVDF. The membranes were then immunoblotted with the indicated specific antibodies. *B*, serum-starved Jurkat T cells were left unstimulated (*lane 1*) or stimulated either with the anti-CD38 mAb antibody, OKT10 (*lane 2*), or with IB4 (*lane 3*), followed by cross-linking with the αmo for 5 min at 37 °C. Rafts were isolated as in *A*. 25-μl aliquots (in sample buffer) of rafts fractions were resolved on 11% SDS-PAGE under non-reducing conditions and transferred to PVDF. Separated proteins were immunoblotted with anti-Sos (*upper panel*), anti-p85α subunit of the PI 3-kinase (*middle panel*), or anti-LAT (*lower panel*) antibodies. Blots from *A* and *B* were scanned, and protein bands were quantified using the NIH Image program 1.62 version. Fold increase in the densitometric units (corrected by area) relative to unstimulated cells is indicated at the *bottom of each lane*. The data are representative of three independent experiments.

Recruitment of Sos and the p85α Regulatory Subunit of the PI 3-Kinase to Membrane Rafts upon CD38 Ligation—To examine whether additional signaling molecules were recruited to rafts upon CD38 engagement, despite the fact that they do not become tyrosine-phosphorylated, Jurkat T cells were stimulated with the anti-CD38 mAb, IB4, followed by cross-linking with the $F(ab')_2$ fraction of a secondary antibody for 3 min. Cells were then lysed in 1% Brij 98 at 37 °C and subjected to sucrose gradient fractionation. The low density raft fractions 2–4 were pooled and concentrated, and proteins were separated by SDS-PAGE under non-reducing conditions and analyzed by Western blot with various specific antibodies. As shown in Fig. 5*A*, we observed that upon CD38 ligation for 3 min the amount of Sos and p85 PI 3-kinase in rafts increased 2- and 14-fold, respectively (Fig. 5*A*, *lane 2 versus lane 1*). These increments appeared to be specific because the relative amounts of Vav and LAT remained unchanged following CD38 engagement, whereas ZAP-70, Lck, CD3-ζ, and CD3-ϵ increments ranged from 1.2- to 1.6-fold over unstimulated cells. Furthermore, a more patent translocation of Sos, and particularly of p85 PI 3-kinase, to rafts was observed at 5 min following CD38 ligation with IB4 (Fig. 5*B*, *lane 3*, *upper* and *middle panels*, respectively). When another anti-CD38 mAb, OKT10, was used to stimulate cells, the translocation of Sos and p85α to rafts also occurred but less efficiently (Fig. 5*B*, *upper* and

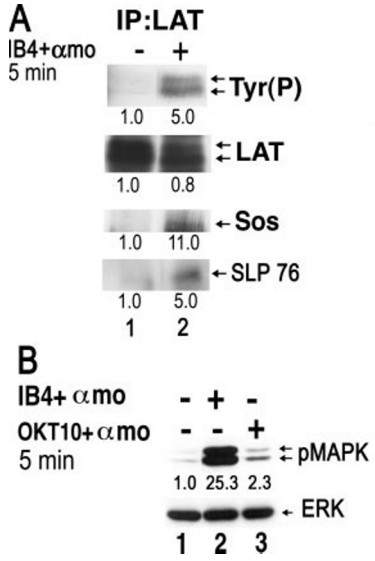

FIG. 6. *A*, recruitment of Sos and SLP-76 by tyrosine-phosphorylated LAT upon CD38 ligation. Jurkat T cells serum-starved overnight (4×10^7 per point) were prepared and stimulated with the anti-CD38 mAb IB4 + αmo for 5 min at 37 °C as described above. Cells were lysed in 1% Nonidet P-40 lysis buffer on ice. Post-nuclear supernatants were subjected to immunoprecipitation (*IP*) of LAT as described under "Experimental Procedures." Immunoprecipitates were separated on 11% SDS-PAGE under reducing conditions and subjected to immunoblotting with an anti-Tyr(P) mAb (*upper panel*). Membrane was then striped and reblotted with antibodies to the indicated proteins (to the *right* of each panel). Fold increase in the densitometric units (corrected by area) relative to unstimulated cells is indicated at the *bottom of each lane*. *B*, CD38-mediated Erk activation. Jurkat cells were left unstimulated (*lane 1*), stimulated with the anti-CD38 mAb antibodies IB4 (*lane 2*), or OKT10 (*lane 3*), followed by cross-linking with the αmo for 5 min at 37 °C. After stimulation cells were immediately lysed in ice-cold 1% Nonidet P-40 lysis buffer. Post-nuclear supernatants were separated on 10% SDS-PAGE under reducing conditions and subjected to immunoblotting with an anti-diphospho-Erk mAb (*upper panel*). Then the filter was stripped and reprobed with an anti-Erk polyclonal antibody (*lower panel*). Fold increase in the densitometric units (corrected by area) relative to unstimulated cells is indicated at the *bottom* of the *upper panel*. The data are representative of three independent experiments.

middle panels, *lane 2*), which correlated with its relatively lower capability of inducing Erk activation (Fig. 6*B*). Note that the anti-p85α mAb used for immunoblotting detected a doublet in CD38-stimulated cells (Fig. 5*B*, *middle panel*, *lanes 2* and *3*). The upper band, which is also present in unstimulated cells (*lane 1*), may correspond to the p85β isoform, which is constitutively associated with lipid rafts in Jurkat T cells (14). Because neither Sos nor p85 PI 3-kinase become tyrosine-phosphorylated upon CD38 engagement (Ref. 30 and data not shown), the data suggested that the recruitment of Sos and p85 PI 3-kinase to raft membranes may reflect the specific interaction of these proteins with raft components, which in turn may facilitate the CD38-mediated activation of the Raf-Erk and PI 3-kinase/Akt signaling pathways.

Recruitment of Sos and SLP-76 to Tyrosine-phosphorylated LAT upon CD38 Engagement—LAT tyrosine phosphorylation and recruitment of Grb2-Sos are important steps for TCR-mediated Ras activation (58). Given that LAT is located in rafts, and Sos is translocated to rafts upon CD38 cross-linking, we addressed the question whether cross-linking of CD38 leads to LAT tyrosine phosphorylation and subsequent recruitment of Sos in Jurkat T cells. To this end, anti-LAT immunoprecipitates from unstimulated or anti-CD38-stimulated cells lysed in 1% Nonidet P-40 were immunoblotted with an anti-Tyr(P) mAb. As shown in Fig. 6*A*, CD38 ligation induced a significant increase in LAT tyrosine phosphorylation (*upper panel*, *lane 2 versus lane 1*). Sos was readily detected in LAT immunoprecipitates from CD38-stimulated cells, and not from unstimulated cells (Fig. 6*A*, *3rd panel*, *lanes 2* and *1*, respectively). Therefore, this result suggests that CD38-mediated tyrosine phosphorylation of LAT promotes the recruitment of Grb2-Sos complexes to rafts. Because another critical role of LAT is to bring SLP-76-Gads complexes, and its associated proteins, to the membrane in a tyrosine phosphorylation manner (59), we next tested whether SLP-76 was recruited to LAT upon CD38 ligation. As shown in Fig. 6*A*, SLP-76 was detected in LAT immunoprecipitates from CD38-stimulated cells (*lower panel*, *lane 2*) and not from unstimulated cells (*lower panel*, *lane 1*), which is in agreement with an active recruitment of SLP-76-Gads to tyrosine-phosphorylated LAT.

Because translocation of Sos to rafts was better induced by the anti-CD38 mAb IB4 than with OKT10, the relative potency of these mAbs to induce Erk activation was studied. As shown in Fig. 6*B*, IB4 mAb induced a higher increase in Erk phosphorylation than OKT10, as expected.

CD38 Ligation Induces Ras Activation Within Rafts—Although translocation of Grb2-Sos complexes into rafts leads to Ras activation upon TCR stimulation (60), and we have demonstrated that CD38 ligation leads to Raf/Erk activation (28, 30, 31), it is not known whether Ras is activated upon CD38 engagement. To determine this possibility, serum-starved Jurkat T cells were stimulated with the anti-CD38 mAb IB4 for 2 and 5 min. Activated GTP-bound Ras was extracted from lysates with a GST fusion protein containing the N-terminal Ras binding domain of Raf (see "Experimental Procedures"). The amount of activated Ras in the pull-outs was determined by immunoblotting with an anti-Ras antibody that recognizes the three main Ras isoforms (H-Ras, N-Ras, and K-Ras). As shown in Fig. 7*A*, CD38 ligation induced a time-dependent activation of Ras, which was stronger at 2 min following stimulation than at 5 min.

In Jurkat T cells the only Ras isoform expressed is N-Ras (61), which potentially could be targeted to lipid rafts via palmitoylation at cysteine 181 (62). To examine whether N-Ras present within rafts become activated upon CD38 engagement, the GTP-Ras pull-down assay was performed in pooled raft fractions from either unstimulated or CD38-stimulated Jurkat T cells. As shown in Fig. 7*B*, CD38 ligation induced activation of Ras within rafts at 2 min following stimulation, as judged by the increase in the amount of GTP-bound Ras recovered in the pull-outs (*lane 2 versus lane 1*). In contrast, not such increase was observed in the non-raft-soluble fraction at this time point (data not shown).

DISCUSSION

In a previous paper (31), we have demonstrated that in T cells CD38 is associated with lipid rafts. However, little is known about the protein composition of CD38-containing rafts and whether specific interactions exist between CD38 and other well characterized raft-associated signaling proteins. By using specific antibodies bound to protein G superparamagnetic microbeads, we have analyzed the distribution pattern of CD38, Lck, CD3-ζ, CD3-ϵ, and LAT in immunoisolated rafts from Jurkat T cells. This study indicates that CD38 is concentrated in a subset of rafts that have relatively high levels of Lck and CD3-ζ, whereas CD3-ϵ and LAT are weakly detected. Moreover, the CD3-ζ and CD3-ϵ subunits seem to be concentrated in a subset highly enriched in Lck and to a lesser extent with LAT. Thus, the distribution pattern of these molecules in CD3-ϵ rafts is very similar to that in Brij 98-resistant immunoisolated CD3-ϵ rafts from a murine T cell line (27). On the other hand, Lck rafts retrieve all the molecules analyzed, whereas LAT rafts are highly enriched in Lck, show intermediate levels of CD3-ζ and CD3-ϵ, and low levels of CD38. There-

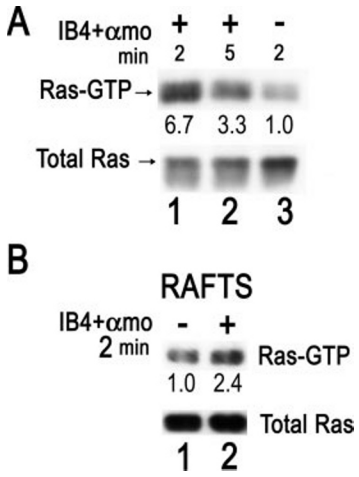

FIG. 7. **CD38 ligation induces Ras activation within rafts.** *A*, $2–4 \times 10^7$ Jurkat T cells, which were starved overnight in 0.1% serum RPMI/HEPES, were left unstimulated (−) or stimulated with the anti-CD38 mAb antibody, IB4, at 5 μg/10^7 cells, followed by cross-linking with the F(ab′)$_2$ fragment of a secondary antibody (*αmo*), for the indicated periods of time, at 37 °C. After stimulation cells were immediately lysed in ice-cold Mg^{2+} lysis buffer (see "Experimental Procedures"). Active GTP-bound Ras was extracted from post-nuclear supernatants with the GST-Raf-Ras-binding domain (*RBD*), coupled to glutathione-agarose, and analyzed by immunoblotting with anti-Ras antibody (clone RAS 10) (*upper panel*). Total Ras was measured by anti-Ras immunoblot analysis of the post-nuclear supernatants (400,000 cell equivalents per lane) (*lower panel*). Fold increase in the GTP-bound Ras relative to unstimulated cells is indicated at the *bottom* of the *upper panel*. The data were previously corrected by dividing the amount of GTP-bound Ras by the amount of total Ras protein detected in the immunoblots. *B*, pooled Brij 98-resistant raft sucrose gradient fractions from unstimulated (*lane 1*) or IB4-stimulated (*lane 2*) Jurkat cells were solubilized in ice-cold Mg^{2+} lysis buffer and processed as above. Fold increase in the GTP-bound Ras (corrected by total Ras content) relative to unstimulated cells is indicated at the *bottom* of the *upper panel*. The data are representative of at least three independent experiments.

fore, there are quantitative and qualitative differences in the protein content of the raft subsets so far studied, although there is also some degree of overlapping, presumably because most of these molecules are part of pre-formed signaling complexes**.**

Recent evidence suggests that LAT and Lck could reside in separate raft domains in human T lymphoblasts (63). Interestingly, in the same report TCR stimulation induced the co-localization of LAT and Lck to 50–100 nm microdomains, which suggested that in these cells the coalescence of LAT- and Lck-containing rafts requires T cell activation. In contrast, the results presented in this report demonstrate that in unstimulated Jurkat T cells raft subsets exist containing Lck, LAT, and the TCR-CD3 complex. Moreover, recent data by Kabouridis (49) show the selective interaction of LAT with the open active form of Lck in lipid rafts from Jurkat T cells, whereas such interaction in the soluble non-raft fraction is minimal. Altogether, these data suggest that in normal T cells the association of LAT with Lck-containing rafts is regulated by TCR signaling, whereas in Jurkat T cells there is a constitutive association of these proteins in the same raft subsets, which may explain why in these cells the TCR-generated signals are amplified more rapidly than in resting T cells.

Within these pre-assembled signaling units, some of these protein complexes are very sensitive to raft disruption, which suggest weak and very likely dynamic interactions, involving protein-protein and protein-lipid interactions. Thus, treatment of the raft membrane vesicles with ODG causes the dissociation of LAT from CD3-ζ and CD3-ϵ immunoprecipitates. Likewise, ODG causes a significant dissociation of Lck from CD38 immunoprecipitates and the complete lost of CD38 from Lck immunoprecipitates. These results could be explained by the selective dissociation of LAT and CD38 from raft membrane vesicles by ODG, whereas Lck, CD3-ζ, and CD3-ϵ remain associated to them (Table I). In this sense, it has been reported in murine T cells that CD38 and Lck could interact directly through the CD38 cytoplasmic tail and the Lck Src homology 2 domain (64). Interestingly, such interaction takes place in cells solubilized in a lysis buffer containing 1% digitonin, which is a mild detergent known to preserve lipid raft-protein interactions (65).

In contrast, other protein complexes are well maintained regardless of using ODG detergent to solubilize rafts, which suggest that they occur primarily via protein-protein interactions. Thus, the associations of Lck with either CD3-ζ or CD3-ϵ are relatively well maintained in the presence of ODG and are detected independently of the antibody used for immunoprecipitation (*i.e.* anti-Lck, anti-CD3-ζ, or anti-CD3-ϵ). These data further support that Lck and the TCR-CD3 complex are tightly associated within the Lck and/or the TCR raft subsets. Since in rafts a small fraction of both CD3-ζ and CD3-ϵ seems to be constitutively phosphorylated (Fig. 4), it is likely that Lck-CD3 association takes place through phosphotyrosine-dependent interactions.

Another protein ensemble, which probably takes place via protein-protein interactions, is the association of CD38 with CD3-ζ. Thus, in the anti-CD38 immunoprecipitates from raft fractions a similar proportion of CD3-ζ remains associated with CD38 independently of the presence or absence of ODG. Moreover, the association of CD38 with CD3-ζ is found in both raft and soluble fractions and in rafts from Lck-deficient cells, which demonstrates that CD38-CD3-ζ interactions can occur independently of raft partitioning of their components, do not require Lck, and are not artifacts of incomplete solubilization. However, in Jurkat T cells there are clear differences in the surface expression of the CD3 subunits and CD38, along with differences in the proportion of each molecule partitioning into rafts, which may dramatically influence the stoichiometry of CD38-CD3-ζ complexes within rafts, or outside them. The results indicate that changes in the surface expression of CD38, CD3-ζ, or both may greatly affect the number of available CD38-CD3-ζ complexes, which in turn may affect the threshold level required to initiate transmembrane signaling through CD38.

Other protein associations, which are stable in 1% Brij 98 but not in 60 mM ODG, are direct, however. Perhaps the best example is the CD3-ζ-CD3-ϵ complexes, which are detected in both raft and soluble fractions. Our data are consistent with the evidence that CD3-ζ is loosely associated to the other TCR-CD3 subunits (66), and therefore its interaction with the other CD3 polypeptide chains is more sensitive to non-ionic detergents than the more tightly associated TCR-$\alpha\beta$·CD3-$\gamma\epsilon$ or TCR-$\alpha\beta$·CD3-$\delta\epsilon$ subcomplexes (50, 67, 68).

CD38 clustering induces tyrosine phosphorylation of Lck, LAT, ZAP-70, and p55 PI 3-kinase within rafts. Moreover, full phosphorylation of CD3-ζ and CD3-ϵ only occurs in raft membranes, as judged by the apparent molecular weight of the different tyrosine-phosphorylated CD3-ζ (23- and 21-kDa forms with a ratio 23:21 higher than 1) and CD3-ϵ forms detected in the anti-Tyr(P) immunoprecipitates. The 21- and/or 23-kDa forms of CD3-ζ may contribute to T cell survival and to T cell responses against pathogens such as bacteria and viruses (69). These data suggest that activation signals initiated in CD38 rafts are rapidly propagated to other raft compartments, where the amplification signaling machinery is present (*i.e.* LAT-enriched rafts, etc.).

CD38-mediated tyrosine phosphorylation of CD3-ζ, CD3-ϵ, ZAP-70, and LAT may be functionally related to the recruit-

ment of Sos and subsequent activation of N-Ras within rafts. In TCR-mediated signaling tyrosine phosphorylation of raft-associated LAT by ZAP-70 may result in an exchange of Sos between the ZAP-70-Grb2-Sos and LAT-Grb2-Sos complexes (60). A similar model is compatible with our observations in Jurkat T cells, where CD38 ligation induces tyrosine phosphorylation of both ZAP-70 and LAT, recruitment of Sos to phospho-LAT (Fig. 6*A*), and targeting of Sos into rafts as well (Fig. 5). Therefore, a pathway leading from CD38 through Ras to Erk requires the formation of a signaling complex made up of the TCR-CD3 (28), Lck (30), ZAP-70 (30, 31), and its downstream effector LAT. In this model, tyrosine phosphorylation of ZAP-70 and LAT are likely to be essential for CD38-induced targeting of Sos into rafts containing Ras. Therefore, as it is pointed out elsewhere, the formation of functional signaling complexes is unlikely to be stabilized solely through interactions with lipid rafts but does require phosphotyrosine-dependent interactions (70–72). In murine T cells, where CD38-mediated LAT tyrosine phosphorylation is weaker than in Jurkat T cells, we favor a model in which the adaptor Shc might have a crucial role (31). In this sense, Shc partitions into rafts following TCR engagement (14), and targeting of Shc to rafts leads to constitutive activation of the Ras/Erk signaling pathway and enhanced TCR signaling (73).

The distinct membrane microlocalization of the different Ras isoforms clearly has important potential consequences for effector interactions and activation of downstream pathways (74). In cell membranes prepared under detergent-free conditions, doubly palmitoylated H-Ras localizes in both lipid raft microdomains and bulk plasma membrane, whereas K-Ras is predominantly present in the bulk disordered membrane (74–76). On the other hand, 75–80% of unipalmitoylated N-Ras is found in non-caveolar lipid raft fractions from N-Ras-transfected COS-7 cells lysed in 0.25% Triton X-100 (77), and in unstimulated Jurkat T cells extracted with 1% Brij 98 at 37 °C, about 13% of N-Ras migrates with lipid rafts (data not shown). Because Ras interaction with lipid rafts is highly sensitive to detergent extraction (74, 75), it is likely that we are underestimating the amount of N-Ras present in lipid rafts. In any case, CD38 ligation with an agonist anti-CD38 mAb causes N-Ras activation within Brij 98-resistant rafts (Fig. 7) and not in soluble fractions. However, the bulk of the Erk activation occurs in the non-raft fractions (Fig. 4), and disruption of raft interactions by treatment with methyl-β-cyclodextrin strongly stimulates CD38-mediated Erk activation (31). Thus, association with raft domains may be involved in the first steps leading to Ras/Erk activation, but rafts do not constitute the final site of activation of this signaling pathway. These data are consistent with the concept that N-Ras may exist in a dynamic equilibrium between lipid rafts and the disordered plasma membrane, as has been demonstrated for doubly palmitoylated H-Ras (74, 76, 78).

In Jurkat T cells the regulatory p85α subunit of the PI 3-kinase is recruited to rafts after CD38 cross-linking, whereas the p85β isoform is constitutively present in rafts. Moreover, a tyrosine-phosphorylated p55α isoform was also present in rafts and became increasingly tyrosine-phosphorylated upon CD38 ligation. Because CD3-ζ and CD3-ϵ are tyrosine-phosphorylated upon CD38 cross-linking (Zubiaur *et al.* (28, 31) and this paper), and these proteins could interact in a phosphorylation-dependent manner with the p85α PI 3-kinase (31, 79, 80), they could target PI 3-kinase to rafts. In addition, binding of PI 3-kinase to the TCR-CD3 *per se* could up-regulate the PI 3-kinase activity (79, 80), presumably by a conformational change as reported previously for other p85-binding proteins (81, 82). Other candidate molecules are LAT, Shc, and Cbl, as these molecules bind p85 (83), and are tyrosine-phosphorylated upon CD38 stimulation (Figs. 4 and 6) (28, 30, 31). An initiating process could occur with molecules such as CD3-ζ and CD3-ϵ, whereas LAT or Shc may responsible for maintaining or amplifying PI 3-kinase activation. Both events are likely important for PI(3,4,5)P_3 generation after CD38 cross-linking. These interactions with lipid rafts are likely to be functionally significant, because in one earlier study we demonstrated that disruption of raft domains by treatment with methyl-β-cyclodextrin prevents the PI 3-kinase/Akt activation mediated by CD38 (31).

In contrast, c-Cbl, which in B cells is related to inhibition of CD38-mediated cell growth (84), becomes tyrosine-phosphorylated exclusively in the non-raft compartment with delayed kinetics in respect to other signaling molecules. Partial tyrosine phosphorylation of CD3-ζ, which has been correlated with partial TCR signaling (52), is also found in the non-raft plasma membrane. Note that in the non-raft fraction the small amount of Lck detected is not associated with CD38, which could explain why full phosphorylation of CD3-ζ does not occur upon CD38 ligation. Therefore, the CD38 present in the disordered, non-raft plasma membrane might be involved in the initiation of inhibitory signals as c-Cbl tyrosine phosphorylation and partial CD3-ζ tyrosine phosphorylation, although we cannot rule out that CD38 ligation within rafts may regulate lateral segregation of inhibitory signaling molecules from rafts to the non-raft compartment. Likewise, lateral segregation of activating signaling molecules from raft to non-raft sites is likely to occur later on, because the bulk of Erk activation is detected somewhere outside the lipid rafts. In summary, this study provides new insights into the mechanisms by which CD38 transduces signals inside the cell, demonstrating that there are two pools of CD38, which differ in their microdomain localization, associated proteins, and distinct signaling outputs.

Acknowledgments—We gratefully acknowledge Dr. José-Manuel Palma from the Estación Experimental del Zaidín (CSIC), Granada, Spain, for sharing knowledge and the invaluable help in sucrose gradient ultracentrifugation experiments. We thank Dr. Balbino Alarcón for the gift of the anti-CD3-ζ antibody 448, Dr. Stephen C. Ley for kindly supplying the anti-ZAP-70 antibody Zap-4, and Dr. Arthur Weiss for providing the JCaM1.6 cells. We also thank Antonio Mérida for expert mAb purification.

REFERENCES

1. Terhorst, C., van Agthoven, A., Le Clair, K., Snow, P., Reinherz, E. L., and Schlossman, S. F. (1981) *Cell* **23,** 771–780
2. Jackson, D. G., and Bell, J. I. (1990) *J. Immunol.* **144,** 2811–2815
3. Malavasi, F., Funaro, A., Roggero, S., Horenstein, A., Calosso, L., and Mehta, K. (1994) *Immunol. Today* **15,** 95–97
4. Deaglio, S., Mallone, R., Baj, G., Arnulfo, A., Surico, N., Dianzani, U., Mehta, K., and Malavasi, F. (2000) *Chem. Immunol.* **75,** 99–120
5. Ferrero, E., Saccucci, F., and Malavasi, F. (2000) *Chem. Immunol.* **75,** 1–19
6. Funaro, A., Ferrero, E., Mehta, K., and Malavasi, F. (2000) *Chem. Immunol.* **75,** 256–273
7. Berthelier, V., Tixier, J. M., Muller-Steffner, H., Schuber, F., and Deterre, P. (1998) *Biochem. J.* **330,** 1383–1390
8. Mehta, K., Shahid, U., and Malavasi, F. (1996) *FASEB J.* **10,** 1408–1417
9. Franco, L., Guida, L., Bruzzone, S., Zocchi, E., Usai, C., and De Flora, A. (1998) *FASEB J.* **12,** 1507–1520
10. Sun, L., Adebanjo, O. A., Koval, A., Anandatheerthavarada, H. K., Iqbal, J., Wu, X. Y., Moonga, B. S., Wu, X. B., Biswas, G., Bevis, P. J., Kumegawa, M., Epstein, S., Huang, C. L., Avadhani, N. G., Abe, E., and Zaidi, M. (2002) *FASEB J.* **16,** 302–314
11. Partida-Sanchez, S., Cockayne, D. A., Monard, S., Jacobson, E. L., Oppenheimer, N., Garvy, B., Kusser, K., Goodrich, S., Howard, M., Harmsen, A., Randall, T. D., and Lund, F. E. (2001) *Nat. Med.* **7,** 1209–1216
12. Simons, K., and Toomre, D. (2000) *Nat. Rev. Mol. Cell. Biol.* **1,** 31–39
13. Brown, D. A., and London, E. (2000) *J. Biol. Chem.* **275,** 17221–17224
14. Xavier, R., Brennan, T., Li, Q., McCormack, C., and Seed, B. (1998) *Immunity* **8,** 723–732
15. Moran, M., and Miceli, M. C. (1998) *Immunity* **9,** 787–796
16. Janes, P. W., Ley, S. C., and Magee, A. I. (1999) *J. Cell Biol.* **147,** 447–461
17. Montixi, C., Langlet, C., Bernard, A. M., Thimonier, J., Dubois, C., Wurbel, M. A., Chauvin, J. P., Pierres, M., and He, H. T. (1998) *EMBO J.* **17,** 5334–5348
18. Cheng, P. C., Brown, B. K., Song, W., and Pierce, S. K. (2001) *J. Immunol.* **166,** 3693–3701

19. Cheng, P. C., Dykstra, M. L., Mitchell, R. N., and Pierce, S. K. (1999) *J. Exp. Med.* **190,** 1549–1560
20. Petrie, R. J., Schnetkamp, P. P., Patel, K. D., Awasthi-Kalia, M., and Deans, J. P. (2000) *J. Immunol.* **165,** 1220–1227
21. Field, K. A., Holowka, D., and Baird, B. (1997) *J. Biol. Chem.* **272,** 4276–4280
22. Deans, J. P., Robbins, S. M., Polyak, M. J., and Savage, J. A. (1998) *J. Biol. Chem.* **273,** 344–348
23. Yang, H., and Reinherz, E. L. (2001) *J. Biol. Chem.* **276,** 18775–18785
24. Ilangumaran, S., Briol, A., and Hoessli, D. C. (1998) *Blood* **91,** 3901–3908
25. Millan, J., Montoya, M. C., Sancho, D., Sanchez-Madrid, F., and Alonso, M. A. (2002) *Blood* **99,** 978–984
26. Yashiro-Ohtani, Y., Zhou, X. Y., Toyo-Oka, K., Tai, X. G., Park, C. S., Hamaoka, T., Abe, R., Miyake, K., and Fujiwara, H. (2000) *J. Immunol.* **164,** 1251–1259
27. Drevot, P., Langlet, C., Guo, X. J., Bernard, A. M., Colard, O., Chauvin, J. P., Lasserre, R., and He, H. T. (2002) *EMBO J.* **21,** 1899–1908
28. Zubiaur, M., Guirado, M., Terhorst, C., Malavasi, F., and Sancho, J. (1999) *J. Biol. Chem.* **274,** 20633–20642
29. Morra, M., Zubiaur, M., Terhorst, C., Sancho, J., and Malavasi, F. (1998) *FASEB J.* **12,** 581–592
30. Zubiaur, M., Izquierdo, M., Terhorst, C., Malavasi, F., and Sancho, J. (1997) *J. Immunol.* **159,** 193–205
31. Zubiaur, M., Fernandez, O., Ferrero, E., Salmeron, J., Malissen, B., Malavasi, F., and Sancho, J. (2002) *J. Biol. Chem.* **277,** 13–22
32. Brown, D. A., and London, E. (1998) *Annu. Rev. Cell Dev. Biol.* **14,** 111–136
33. Pralle, A., Keller, P., Florin, E. L., Simons, K., and Horber, J. K. (2000) *J. Cell Biol.* **148,** 997–1008
34. Varma, R., and Mayor, S. (1998) *Nature* **394,** 798–801
35. Deaglio, S., Dianzani, U., Horenstein, A. L., Fernandez, J. E., Kooten, C. V., Bragardo, M., Funaro, A., Garbarino, G., Virgilio, F. D., Banchereau, J., and Malavasi, F. (1996) *J. Immunol.* **156,** 727–734
36. Straus, D. B., and Weiss, A. (1992) *Cell* **70,** 585–593
37. Funaro, A., Monte, L. B. D., Dianzani, U., Forni, M., and Malavasi, F. (1993) *Eur. J. Immunol.* **23,** 2407–2411
38. Sancho, J., Franco, R., Chatila, T., Hall, C., and Terhorst, C. (1993) *Eur. J. Immunol.* **23,** 1636–1642
39. Poncelet, P., and Carayon, P. (1985) *J. Immunol. Methods* **85,** 65–74
40. Iyer, S. B., Hultin, L. E., Zawadzki, J. A., Davis, K. A., and Giorgi, J. V. (1998) *Cytometry* **33,** 206–212
41. Zubiaur, M., Sancho, J., Terhorst, C., and Faller, D. V. (1995) *J. Biol. Chem.* **270,** 17221–17228
42. Ilangumaran, S., Arni, S., van Echten-Deckert, G., Borisch, B., and Hoessli, D. C. (1999) *Mol. Biol. Cell* **10,** 891–905
43. Brown, D. A., and Rose, J. K. (1992) *Cell* **68,** 533–544
44. Melkonian, K. A., Chu, T., Tortorella, L. B., and Brown, D. A. (1995) *Biochemistry* **34,** 16161–16170
45. Millan, J., Cerny, J., Horejsi, V., and Alonso, M. A. (1999) *Tissue Antigens* **53,** 33–40
46. Delgado, P., Fernandez, E., Dave, V., Kappes, D., and Alarcon, B. (2000) *Nature* **406,** 426–430
47. Ilangumaran, S., and Hoessli, D. C. (1998) *Biochem. J.* **335,** 433–440
48. Roper, K., Corbeil, D., and Huttner, W. B. (2000) *Nat. Cell Biol.* **2,** 582–592
49. Kabouridis, P. S. (2003) *Biochem. J.* **371,** 907–915
50. Exley, M., Wileman, T., Mueller, B., and Terhorst, C. (1995) *Mol. Immunol.* **32,** 829–839
51. van Oers, N. S., Tohlen, B., Malissen, B., Moomaw, C. R., Afendis, S., and Slaughter, C. A. (2000) *Nat. Immun.* **1,** 322–328
52. Sloan-Lancaster, J., Shaw, A. S., Rothbard, J. B., and Allen, P. M. (1994) *Cell* **79,** 913–922
53. Madrenas, J., Wange, R. L., Wang, J. L., Isakov, N. A., Samelson, L. E., and Germain, R. N. (1995) *Science* **267,** 515–518
54. Kersh, E. N., Shaw, A. S., and Allen, P. M. (1998) *Science* **281,** 572–575
55. Hartley, D., and Corvera, S. (1996) *J. Biol. Chem.* **271,** 21939–21943
56. Chan, A. C., Dalton, M., Johnson, R., Kong, G. H., Wang, T., Thoma, R., and Kurosaki, T. (1995) *EMBO J.* **14,** 2499–2508
57. Lupher, M. L., Jr., Rao, N., Eck, M. J., and Band, H. (1999) *Immunol. Today* **20,** 375–382
58. Finco, T. S., Kadlecek, T., Zhang, W., Samelson, L. E., and Weiss, A. (1998) *Immunity* **9,** 617–626
59. Liu, S. K., Fang, N., Koretzky, G. A., and McGlade, C. J. (1999) *Curr. Biol.* **9,** 67–75
60. Salojin, K. V., Zhang, J., Meagher, C., and Delovitch, T. L. (2000) *J. Biol. Chem.* **275,** 5966–5975
61. Makover, D., Cuddy, M., Yum, S., Bradley, K., Alpers, J., Sukhatme, V., and Reed, J. C. (1991) *Oncogene* **6,** 455–460
62. Prior, I. A., and Hancock, J. F. (2001) *J. Cell Sci.* **114,** 1603–1608
63. Schade, A. E., and Levine, A. D. (2002) *J. Immunol.* **168,** 2233–2239
64. Cho, Y. S., Han, M. K., Choi, Y. B., Yun, Y., Shin, J., and Kim, U. H. (2000) *J. Biol. Chem.* **275,** 1685–1690
65. van't Hof, W., and Resh, M. D. (1999) *J. Cell Biol.* **145,** 377–389
66. Rodriguez-Tarduchy, G., Sahuquillo, A. G., Alarcon, B., and Bragado, R. (1996) *J. Biol. Chem.* **271,** 30417–30425
67. Sancho, J., Chatila, T., Wong, R. C., Hall, C., Blumberg, R., Alarcon, B., Geha, R. S., and Terhorst, C. (1989) *J. Biol. Chem.* **264,** 20760–20769
68. San Jose, E., Sahuquillo, A. G., Bragado, R., and Alarcon, B. (1998) *Eur. J. Immunol.* **28,** 12–21
69. Pitcher, L. A., Young, J. A., Mathis, M. A., Wrage, P. C., Bartok, B., and Van Oers, N. S. (2003) *Immunol. Rev.* **191,** 47–61
70. Guirado, M., de Aos, I., Orta, T., Rivas, L., Terhorst, C., Zubiaur, M., and Sancho, J. (2002) *Biochem. Biophys. Res. Commun.* **291,** 574–581
71. Bunnell, S. C., Hong, D. I., Kardon, J. R., Yamazaki, T., McGlade, C. J., Barr, V. A., and Samelson, L. E. (2002) *J. Cell Biol.* **158,** 1263–1275
72. Hartgroves, L. C., Lin, J., Langen, H., Zech, T., Weiss, A., and Harder, T. (2003) *J. Biol. Chem.* **278,** 20389–20394
73. Plyte, S., Majolini, M. B., Pacini, S., Scarpini, F., Bianchini, C., Lanfrancone, L., Pelicci, P., and Baldari, C. T. (2000) *Oncogene* **19,** 1529–1537
74. Prior, I. A., Harding, A., Yan, J., Sluimer, J., Parton, R. G., and Hancock, J. F. (2001) *Nat. Cell Biol.* **3,** 368–375
75. Song, K. S., Li, S., Okamoto, T., Quilliam, L. A., Sargiacomo, M., and Lisanti, M. P. (1996) *J. Biol. Chem.* **271,** 9690–9697
76. Roy, S., Luetterforst, R., Harding, A., Apolloni, A., Etheridge, M., Stang, E., Rolls, B., Hancock, J. F., and Parton, R. G. (1999) *Nat. Cell Biol.* **1,** 98–105
77. Matallanas, D., Arozarena, I., Berciano, M. T., Aaronson, D. S., Pellicer, A., Lafarga, M., and Crespo, P. (2003) *J. Biol. Chem.* **278,** 4572–4581
78. Hancock, J. F. (2003) *Nat. Rev. Mol. Cell. Biol.* **4,** 373–384
79. Exley, M., Varticovski, L., Markus, P., Sancho, J., and Terhorst, C. (1994) *J. Biol. Chem.* **269,** 15140–15146
80. de Aós, I., Metzger, M. H., Exley, M., Dahl, C. E., Misra, S., Zheng, D., Varticovski, L., Terhorst, C., and Sancho, J. (1997) *J. Biol. Chem.* **272,** 25310–25318
81. Shoelson, S. E., Sivaraja, M., Williams, K. P., Hu, P., Schlessinger, J., and Weiss, M. A. (1993) *EMBO J.* **12,** 795–802
82. Buhl, A. M., and Cambier, J. C. (1997) *Immunol. Rev.* **160,** 127–138
83. Wange, R. L. (2000) *Science STKE* http://www.stke.org/cgi/content/full/OC_sigtrans;2000/RE1
84. Kitanaka, A., Ito, C., Nishigaki, H., and Campana, D. (1996) *Blood* **88,** 590–598